Perceptual Learning as a Rehabilitation Approach to Enhance Motion Processing in Maculopathy Patients

Célia Michaud, Cynthia Faurite, Jade Guénot, Mathilde Gallice, Christophe Chiquet, Nathalie Vayssière, Isabelle Berry, Yves Trotter, Robin Baurès, Maxime Rosito, et al.

Perceptual Learning as a Rehabilitation Approach to Enhance Motion Processing in Maculopathy Patients

Célia Michaud,[1] Cynthia Faurite,[2] Jade Guénot,[1] Mathilde Gallice,[3] Christophe Chiquet,[3] Nathalie Vayssière,[1] Isabelle Berry,[1] Yves Trotter,[1] Robin Baurès,[1] Maxime Rosito,[1] Vincent Soler,[1] Carole Peyrin,[2] and Benoit R. Cottereau[1,4]

[1]University Toulouse, CNRS, CerCo, Toulouse, France
[2]University Grenoble Alpes, University Savoie Mont Blanc, CNRS, LPNC, Grenoble, France
[3]Department of Ophthalmology, Grenoble Alpes University Hospital, Grenoble, France
[4]IPAL, CNRS IRL, Singapore, Singapore

Correspondence: Célia Michaud, CerCo UMR 5549, CNRS - Université Toulouse III, Pavillon Baudot CHU Purpan, Toulouse 31052, France; celia.michaud@cnrs.fr.
Benoit Cottereau, CerCo UMR 5549, CNRS - Université Toulouse III, Pavillon Baudot CHU Purpan, Toulouse 31052, France; benoit.cottereau@cnrs.fr.

CM and CF contributed equally to this work.
CP and BRC are co-senior authors on this work.

Received: October 7, 2025
Accepted: February 8, 2026
Published: March 26, 2026

Citation: Michaud C, Faurite C, Guénot J, et al. Perceptual learning as a rehabilitation approach to enhance motion processing in maculopathy patients. *Invest Ophthalmol Vis Sci.* 2026;67(3):52. https://doi.org/10.1167/iovs.67.3.52

Purpose. Macular degeneration (MD) is a disease affecting the central retina and significantly impairing vision. Given the absence of a cure, rehabilitation strategies are vital for enhancing visual perception.

Methods. This study introduces a perceptual learning (PL) protocol for MD patients, focusing on improving motion perception, a key ability for navigating environments and social interactions. Patients underwent four weeks of motion discrimination training, with pretraining and post-training functional magnetic resonance imaging scans to study the underlying neural mechanisms. We also assessed generalization to an untrained multiobject tracking task in a subset of participants. A control group, matched by age and gender with simulated scotomata, followed the same procedures.

Results. Results in both groups indicated improved motion discrimination and increased responses in the human middle temporal complex (hMT+), a critical neural hub for motion processing. Improvements in the multiobject tracking task suggested transferable learning effects.

Conclusions. These findings highlight perceptual learning as a promising rehabilitation strategy for MD and potentially other eye conditions.

Keywords: macular degeneration, perceptual learning, neuroimaging, motion processing, aging

Macular degeneration (MD) is a chronic and irreversible condition characterized by the progressive loss of central vision owing to retinal damage. Currently affecting an estimated 196 million people worldwide, this number is expected to rise to 288 million by 2040, driven by the aging global population.[1] AMD is the most prevalent form of MD, typically occurring in individuals aged more than 60 years. However, other forms, such as Stargardt disease (STG), a genetic variant of MD, can affect individuals during their teenage years or later in life. All forms of MD result in reduced visual acuity and contrast sensitivity, significantly impacting patients' quality of life by impairing recognition and mobility.[2,3]

Given the current lack of a cure for MD, it is essential to develop rehabilitation strategies aimed at preserving or improving patients' visual perception for daily activities. Perceptual learning (PL), which involves the long-term enhancement of skills through the tuning of neural populations in sensory cortices via training or experience,[4] offers promising avenues in this regard.[5] PL has proven effective not only in older adults,[6–8] but also in clinical populations with various eye conditions, including presbyopia,[9] amblyopia,[10] or even retinitis pigmentosa (RP).[11] Despite the difficulties in organizing multiple training sessions for MD patients, who are typically elderly and face mobility challenges, the few studies that have applied PL to this population consistently report performance improvements and a generalization of learning to untrained visual tasks using protocols based on reading,[12,13] contrast discrimination[14] or lateral masking.[15] For example, Plank et al. (2014)[16] found that training MD patients on texture discrimination also enhanced their Vernier acuity. They further explored the influence of PL on brain activations using functional magnetic resonance imaging (fMRI) and observed modest, although not significant, changes in areas V1, V2, and V3 with training (Plank et al., 2014[16]; see also Rosengarth et al., 2013,[17] where the training focused on stabilizing eye fixation rather than using a perceptual task). Because their training task primarily engages the early visual cortex,[18] it is plausible that the neural effects were limited, as the persistence

of plasticity in area V1 of MD patients is far from being confirmed.[19,20] None of the other PL studies mentioned above measured brain responses, possibly because patients often have MRI contraindications.

In the current study, we investigated whether PL training can enhance motion perception in MD patients. Motion perception is a fundamental cognitive function permitting us to navigate through our environment,[21] interact with moving objects,[22] and engage with other individuals.[23] Enhancing this skill in patients who depend exclusively on their peripheral vision could significantly improve their autonomy and daily functioning. To achieve this, we used a motion direction discrimination task, which has been previously shown to improve perceptual thresholds in both monkeys[24] and humans with normal vision[25] through a modulation of neural activations (in the middle temporal area [MT] for macaques and in its human homologous area [hMT+]). There are several reasons to believe that such a protocol could be effective in MD patients. First, it has been demonstrated that PL can still enhance motion perception in older adults[26,27] and in some clinical populations with eye diseases.[28] Second, multiple studies have shown the existence of plasticity mechanisms in motion-selective areas after central vision loss. For instance, Burnat et al. (2017)[29] reported enhanced neuronal activity in the posteromedial lateral suprasylvian area of adult cats (the homologue of primate cortical area MT; see Villeneuve et al., 2006[30]) following a central retinal lesion (see also Shao et al. [2013][31] for similar results in the MT area of one macaque monkey using fMRI). Interestingly, these enhancements were accompanied by improvements in motion perception. In humans, a recent study found higher functional connectivity between hMT+ and early visual areas responsive to peripheral vision in MD patients.[32]

Here, a group of MD patients underwent 12 training sessions lasting approximately 1 hour on the aforementioned motion discrimination task to evaluate potential improvements in their performance. These sessions were supplemented with pretraining and post-training fMRI recordings to explore the neural mechanisms underlying PL in this case, particularly within motion-selective cortical areas such as hMT+. Additionally, we examined whether the training effects generalized to a more complex motion task involving multiple object tracking (MOT) in a subset of participants. Because the processing of peripheral vision may differ between MD patients and participants with normal vision owing to neural plasticity mechanisms involved in adaptation to central vision loss, we replicated all measurements in a group of age- and gender-matched control participants for comparison. In these controls, the central visual field was masked using simulated scotomas that matched the positions and dimensions of those observed in the corresponding MD patients (see Methods).

Methods

Participants

Eleven patients with maculopathy were recruited from the Retina Center of Purpan Hospital in Toulouse and the Ophthalmology Center of Grenoble Hospital (Table 1). Among them, eight had AMD and three had late-onset STG. All exhibited dense central bilateral scotomas (with MD5, MD6, and STG1 showing foveal sparing) and at least one stable preferred retinal locus (PRL), without other visual pathologies or severe general conditions. Additionally, 11 age- and gender-matched control participants with normal or corrected-to-normal vision and no long-term illnesses were recruited. The age differences between patients and controls were all within 2 years, except for the control of MD2 (81 years) and MD6 (79 years) who were both 75 years old. All participants completed the Mini-Mental State Examination and the Beck Depression Inventory-II (BDI-II) to assess cognitive functions and psychological states, respectively. We made sure that all participants had a score of 23 or greater for the Mini-Mental State Examination and lower than 19 for the BDI-II. Patients' visual function perception was evaluated using the National Eye Institute's Visual Function Questionnaire (VFQ-25).[33] Written informed consent was obtained, and the protocol was approved by the French Ethics Committee of Sud Méditerranée IV (2022-00957-36).

For each participant, we identified the eye with better acuity using Sloan letters from the Freiburg Visual Acuity Test.[34] This eye was chosen for stimulation, and the other eye was patched. An exception occurred with participant MD2, where the other eye was stimulated because the eye with the best acuity lacked a PRL (described in Scotoma Size and Localization of the PRL).

Scotoma Size and Localization of the PRL

To ensure visual input consistency between each MD patient and their matched control, we simulated a central scotoma in the controls. This artificial scotoma mirrored the size and position observed in their paired patients (further details are provided in Artificial Scotoma for Control Participants). Initially, this process involves determining the scotoma size for each patient and identifying the new retinal fixation point they use. To achieve this, an ophthalmologist delineated each patient's scotoma border on autofluorescence images of the eye fundus, with the help of the optical coherence tomography (OCT) data (Fig. 1A). The scotoma area, measured in square degrees of visual angle, was extracted to compute the simulated scotoma for age- and gender-matched controls (discussed in Artificial Scotoma for Control Participants). In case of foveal sparing (as seen with patients MD5, MD6, and STG1), gaze direction was also centered for control participants. Patients with MD typically develop a peripheral neofixation known as a PRL. To locate their PRL, we followed a procedure from previous studies (for details, see Guénot et al. [2022][35] or Michaud et al. [2025][36]). Patients focused on the center of a screen while we performed spectral-domain OCT (Fig. 1B). This process was repeated three times with short breaks to ensure stable retinal fixation measurements. The PRL coordinates in degrees of visual angle were then referenced relative to the fovea, visible on OCT images (Fig. 1C).

Despite the presence of a central scotoma, STG1 showed foveal sparing and maintained foveal fixation in both eyes, a phenomenon commonly observed in late-onset STG.[37] MD5 and MD6 also fixated near the fovea.

Artificial Scotoma for Control Participants

For each control participant, the visual field was masked with an artificial scotoma centered on the fovea (except in CTRL2 and CTRL3, where it was shifted to the left because MD2's and MD3's scotoma occupied a larger portion of the left visual hemifield). The size of this artificial scotoma

Table 1. Characteristics of MD Patients and Age-Matched Controls Included in the Study

Patients	**MD1**	**MD2**	**MD3**	**MD4**	**MD5**	**MD6**	**MD7**	**MD8**	**STG1**	**STG2**	**STG3**
Sex	Female	Male	Female	Male	Male	Male	Male	Female	Female	Male	Male
Age, years	75	81	66	73	75	79	74	73	50	69	25
Visual acuity											
Left eye	0.14	0.03	0.6	0.23	0.05	0.08	0.1	0.12	0.39	0.24	0.46
Right eye	0.15	0.48	0.23	0.22	0.23	0.11	0.07	0.53	0.7	0.25	0.77
Tested eye	Left	Right	Left	Left	Right	Right	Left	Right	Left	Right	Right
fMRI	Yes	Yes	Yes	Yes	Yes	Yes	No	No	Yes	Yes	Yes
MOT	Yes	Yes	Yes	No	No	Yes	No	Yes	No	No	No
Atrophy area (mm^2)	23.08	7.29	13.95	25.44	24.72	8.6	21.12	0.1	6.99	9.09	1.82
Scotoma radius (°)	9.72	5.3	7.31	9.84	6.15 12.31*	5.7	8.25	0.62	5.18	5.87	2.64
PRL polar angle θ (°)	152.6	−36.1	−22.7	180	28.5	−158.2	−170.6	−90	0	90	−84.2
PRL eccentricity ρ (°)	10.4	1.1	2.1	9.58	0.9	1.02	8.8	2.9	0	5.22	6.77
PRL coordinates (μm)	−3239; 1370	245; −179	565; −236	−2761; 0	239; 130	−272; −109	−2499; −410	0; −835	0; 0	0; 1503	196; −1941
PRL coordinates (°)	−9.2; 4.76	0.85; −0.62	1.96; −0.82	−9.58; 0	0.83; 0.45	−0.95; 0.38	−8.68; −1.43	0; −2.9	0; 0	0; 5.22	0.68; −6.74
Controls	**CTRL1**	**CTRL2**	**CTRL3**	**CTRL4**	**CTRL5**	**CTRL6**	**CTRL7**	**CTRL8**	**CTRLSTG1**	**CTRLSTG2**	**CTRLSTG3**
Gender	Female	Male	Female	Male	Male	Male	Male	Female	Female	Male	Male
Age, years	74	75	67	71	77	75	76	70	52	68	26
Visual acuity											
Left eye	1.56	1.06	1.11	1.27	0.96	1.99	1.44	1.44	1.31	1.43	>2
Right eye	1.8	1.11	0.61	1.73	1.71	1.74	0.73	1.32	0.99	2	>2
Tested eye	Right	Right	Left	Left	Left	Right	Left	Right	Left	Right	Right

Precisions about the city where the recordings took place (T for Toulouse, G for Grenoble), their diagnosis (MD for AMD, STG for late-onset STG), whether they took part in the fMRI recordings and/or in the MOT task, the area of their retinal atrophy, the size of their scotoma as well as the polar (θ: angles, in degrees and ρ: eccentricities, in degrees of visual angle) and cartesian coordinates of the PRL, the decimal visual acuity for the left (LE) and right (RE) eye provided. It should be noted that because MD5 had an elongated scotoma, we used an ellipse rather than a disk for the artificial scotoma of his control. In this case, the two values provided in the 'scotoma radius' column (marked by an asterisk) provide the lengths of the ellipse semiminor and semimajor axes.

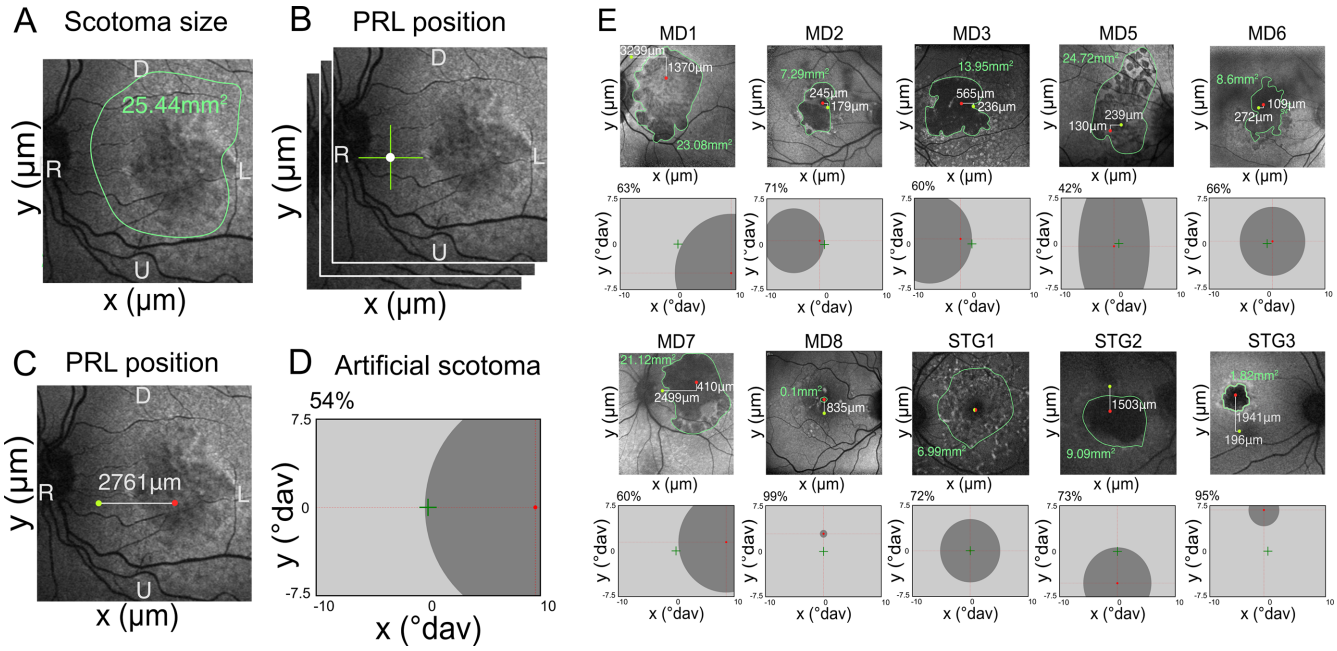

Figure 1. Ophthalmology data measured in patients and associated artificial scotomas used in their age and gender-matched controls. (**A–D**) Estimation of the scotoma size and PRL position in one typical patient (MD4). (**A**) The border of the scotoma (*green*) is delineated from an autofluorescence image of the eye fundus and the associated surface is used to calculate the radius of the scotoma in degrees of visual angle, given that 288 µm on the image corresponds with 1 degree of visual angle. (**B**) Patients had to fixate a central light and we measured the *x* and *y* positions of their PRL with spectral domain OCT (Spectralis OCT; Heidelberg Engineering, Heidelberg, Germany). This process was repeated three times and the average measure provided the final coordinates. (**C**) Position of the measured PRL (*green*) with respect to the fovea (*red*) on the eye fundus. (**D**) From the surface of the scotoma and the position of the PRL, it is possible to simulate the patient's visual field. During the motion direction discrimination task and the associated fMRI experiments, MD patients were instructed to fixate a central cross (*green*) with their PRL. Controls had to fixate a *red cross* at the position corresponding to their paired patient's fovea while an artificial scotoma was displayed in *dark gray*. The *dotted lines* (not shown during the experiments) specify the vertical and horizontal meridians. (**E**) Ophthalmology data (scotoma size and position of the PRL with respect to the fovea) measured in the other patients (*upper rows*) and artificial scotomas in their controls. All retinal images in this figure have been inverted horizontally to be aligned with the visual field. The letters on eye fundus and OCT images specify the orientation of the images. D, down; L, left; R, right; U, up.

matched that of the corresponding patient (see Guénot et al. [2022][35]). Control participants fixated on a cross at their paired patient's foveal position (*red cross* in Fig. 1D), placing the screen center in their peripheral vision at the patient's PRL location. All artificial scotomas were circular, except for CTRL5, which used an ellipse to match the elongated scotoma shape of MD5. This procedure ensured that the position and area of the occluded visual field were consistent between each patient and their control, providing comparable visual inputs.[35]

Protocol Overview

The whole protocol was part of a multicentric project between the CerCo (Toulouse) and LPNC (Grenoble) laboratories and included three different parts distributed over a period of about 6 weeks: a series of pretests, 12 sessions of PL, and a series of post-tests (Fig. 2). The pretests and post-tests consisted of a motion direction discrimination task. These psychophysical measurements were complemented by fMRI recordings in nine MD patients and their control subjects. The only participants who did not undergo fMRI were MD7 and MD8, owing to MRI contraindications, along with their respective controls (CTRL7 and CTRL8). It is important to note that the fMRI activations, along with their associated behavioral performance obtained during these pretests, have been thoroughly detailed in a previous study by our group, which focused on motion processing in patients with maculopathy but did not address the issue of PL.[36] After the pretests, all participants completed 12 training sessions over 4 weeks using the same motion direction discrimination task as in the pretraining and post-tests. To determine whether the effects of training generalize to other types of motion perception, 5 of our 11 MD participants also performed a MOT task during the pretest and the post-tests (but not during the PL sessions). We first describe the experimental setup for the motion direction discrimination task, which was used both to train participants and to assess their motion perception during pretraining and post-training tests. Next, we outline the protocol for our fMRI measurements, aimed at characterizing cortical responses to motion before and after training. Finally, we present the setup for the MOT task, designed to evaluate whether the effects of PL generalize to other motion processing tasks.

Experimental Protocol for Estimating Motion Direction Discrimination Thresholds During Pretraining and Post-training Tests and PL Sessions

All psychophysical sessions, including the pretraining and post-training psychophysical tests and the PL sessions, were conducted in the same experimental rooms. During these sessions, participants were seated in a chair with their head placed in a head support device clamped to the table, equipped with chin and forehead supports. The screen was either a large convex screen in Toulouse (58.1 × 43.8

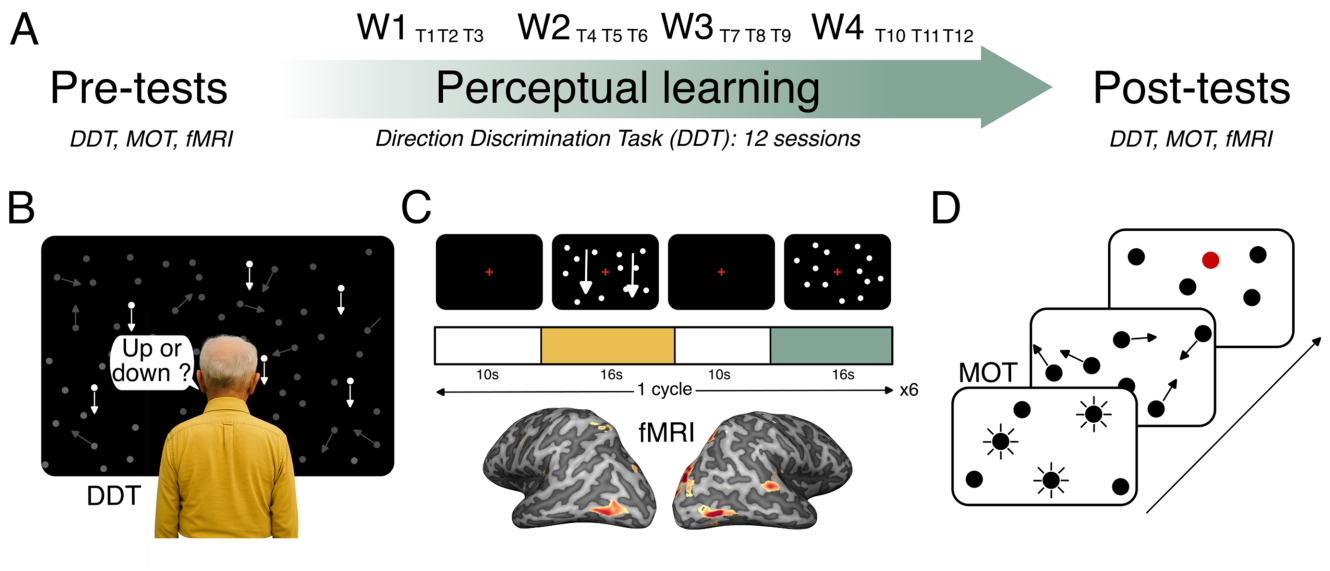

Figure 2. Protocol overview. (**A**) The protocol included three distinct parts distributed over a period of 6 weeks: a series of pretests, 12 sessions of PL (3 sessions a week during 4 weeks) and a series of post-tests, which took place within 2 weeks after the training. During the pretests and post-tests, each participant performed a motion direction discrimination task (DDT). Subsets of participants also underwent fMRI recordings and an additional psychophysical task (see more details in the text). During the PL phase, all participants performed 12 sessions (T1–T12) of the motion direction discrimination task (3 runs). Performance was averaged over each week (W1–W4). (**B**) During these sessions, participants had to report the perceived motion direction of the stimuli (either upward or downward). We manipulated motion coherence and estimated thresholds corresponding with 80% of correct detections. Signal dots are shown in *white* and noise dots in *gray* for better visibility on the figure (all the dots were white during the experiment). During all the recordings, participants had to fixate a red cross that was central for patients (who used their PRL) and at the position corresponding to their paired patient's fovea for controls. The picture of the participant was generated using AI. (**C**) During fMRI recordings, blocks of translational motion (white dots moving either upward or downward on a black background) alternated with blocks of static dots. These blocks were separated by periods of baseline (a black screen). Participants had to fixate a red cross during all the recordings. (**D**) During the MOT task, black disks were displayed on a white screen and participants were instructed to keep track of multiple target disks for 10 seconds. Depending on the trial, we either used three targets among six disks (as illustrated here) or four targets among eight disks. Target discs flickered for 2 seconds before the beginning of each trial. At the end of each trial, a disk became red and participants had to report whether this disk was a target or not.

degrees of visual angle; refresh rate, 60 Hz; resolution, 1024 × 768 pixels) at a viewing distance of 180 cm or a computer screen in Grenoble (48.6 × 30.7 degrees of visual angle; refresh rate, 60 Hz; resolution, 1900 × 1200) at a viewing distance of 55 cm. The height of the chair was adjusted to equalize the height of their eyes with the center of the screens. During all experiments, participants were asked to maintain fixation on a central cross monocularly while the other eye was patched (see Artificial Scotoma for Control Participants).

Motion stimuli were adapted from the experimental protocol of a previous electrophysiological study.[38] They consisted of translational patterns based on random dot kinematograms (Fig. 2B) generated with Matlab (R2017a). The random dot kinematogram consisted of nonoverlapping white dots with a diameter of 0.2 degrees of visual angle moving on a dark background with a contrast of 100% and with a velocity of 7°/s which, corresponds with the average preferred speed of neurons in macaque MT. The density of dots was 0.3945 dots per degree of visual angle. Dots were immediately respawned at a random location if they reached the border of the screen. These stimuli were also adapted for fMRI recording (see Experimental Protocol for fMRI Recordings During Pretraining and Post-training Tests).

A forced binary decision task was used to estimate motion discrimination thresholds. Stimuli were presented in blocks of 64 trials. Each block lasted approximately 3 minutes. Each trial started with the presentation of the stimulus for 200 ms. Participants had to report whether the motion of the stimulus was upward or downward. They were instructed to respond as quickly as possible while maximizing their performance. Responses reported after 2 seconds were considered incorrect. After each trial, an auditory feedback indicated whether the chosen direction was correct or not. During each block, we manipulated motion coherency (i.e., the percentage of dots moving along the same direction while the other dots had random directions) and estimated the thresholds corresponding with 80% of correct detection using an adaptive Bayesian approach (QUEST, see Watson & Pelli [1983][39]), which allows for robust estimations with a limited number of trials (see Guénot et al. [2022][35]). Participants completed four blocks during the pretraining and post-training measurements and three blocks during each PL session. The first block during the pretraining and post-training measurements was considered as a training and not included in the analyses. Breaks were included (3 minutes on average) between blocks to reduce fatigue. Each training session was completed in approximately 20 minutes.

Experimental Protocol for fMRI Recordings During Pretraining and Post-training Tests

fMRI recordings were done on a different day and after behavioral pre tests. In Toulouse, stimuli were projected on a screen with a resolution of 1024 × 768 pixels at a viewing distance of 90 cm, visible within the MRI scanner thanks to

an angled mirror. In Grenoble, the resolution of the screen was 1360 × 768 pixels and the viewing distance was 183 cm. In both MRI platforms, the size of the stimuli were 20 × 15 degrees of visual angle. We used a block design fMRI paradigm (Fig. 2C). One run was 312 seconds long and divided into six identical cycles lasting for 52 seconds. Each cycle started with a baseline period of 10 seconds, during which only a red fixation cross of 1 degree of visual angle was displayed on a black screen. It was followed by a block of 16 seconds of uniform motion, then by another 10 seconds of baseline, and finally by a block of 16 seconds with static dots. In motion blocks, a new pattern of translational motion during which all the dots (defined using the same properties as for the motion direction discrimination task) moved either upward or downward was presented every 2 seconds. These patterns lasted 1.8 seconds and were separated by short periods (0.2 seconds), during which the screen went black and only the fixation cross was presented. The same principle was applied during the blocks of static dots (a new pattern was displayed for 1.8 seconds every 2.0 seconds). We used the software EventIDE (Okazolab) to develop the stimuli and synchronize the display of the stimuli with the acquisition of the functional data. No eye-tracking recording was used during the scan; therefore, to ensure that participants were correctly gazing at the red cross, they were instructed to press a button on a gamepad whenever a white circle appeared around the cross. This circle was only displayed for 200 ms and at random times throughout the acquisition. Despite this short duration, all participants performed the task well. We, therefore, kept all of the runs for further analysis.

(f)MRI Recordings

Independent of the location of acquisition, all fMRI recordings were performed using a 3 Tesla clinical MR scanner (Philips Achieva). Both MRI platforms are also equipped with the same MR hardware configuration (with Quasar Dual gradient system and dStream architecture supporting multiband-accelerated acquisitions, 32-channel head coil) and were run using the same software version (R5.7.1). This permitted us to minimize the differences between the recordings performed in the two cities. Two high-resolution anatomical images of each participant's brain were acquired using a T1-weighted magnetization-prepared rapid gradient-echo sequence (repetition time, TR = 8.1 ms; echo time, TE = 3.7 ms, flip angle = 8°; field of view, 240 × 240 mm; voxel size = 1 × 1 × 1 mm; 170 sagittal slices acquired in an interleaved order). These anatomical images were first co-registered and then averaged together to be used as a reference to which the functional images from all the experiments were aligned. Functional images were collected with a T2*-weighted gradient-echo echoplanar imaging sequence (TR = 2000 ms, TE = 30 ms, flip angle = 75°, SENSE factor = 1.6; multiband = 3; field of view, 224 × 224 mm; matrix size: 112 × 110 mm; voxel size = 2 × 2 × 2 mm, 63 transverse slices). On average, we recorded three runs per participant (a few did two or four runs).

(f)MRI Data Analyses

The preprocessing of fMRI data included slice timing correction, three-dimensional motion correction using trilinear/sinc interpolation, and a linear trend followed by a high-pass filtering using Fourier analysis with a cut-off at three cycles. The preprocessing, as well as further analyses, were both performed using the BrainVoyager software (v23, Brain Innovation, Maastricht, the Netherlands).[40] The functional data was then co-registered on the anatomy for each participant. Both functional and anatomical data were brought into the ACPC space by using cubic spline interpolation and then transformed into standard Talairach space.[41] Finally, the volume time courses were spatially smoothed at 4 mm full width at half maximum. Individual analyses were conducted on each node of the participants' cortical tessellations by fitting a general linear model to the corresponding blood oxygen level-dependent (BOLD) signal. The model included two main regressors representing the experimental conditions: uniform motion (either upward or downward) and control (static dots). These regressors were convolved with a model of the human hemodynamic response function. Additionally, eight regressors of noninterest were included: six for head motion parameters estimated during motion correction and two for time-courses within the ventricles and white matter to reduce data noise (see e.g., Audurier et al. [2022][42]). For each participant, beta weights from the general linear model were used for univariate analyses (t-scores) at the whole-brain level. Results are displayed on inflated surfaces, segmented from white and gray matter, and cerebrospinal fluid, with statistical maps thresholded at a P value of $<10^{-3}$ (uncorrected), common in individual-level fMRI analysis (see, e.g., Aedo-Jury et al., 2020).[43] Group-level analyses were performed within independently defined regions of interest (ROIs), represented by spheres in volumetric space centered on Talairach coordinates from previous studies for areas hMT+,[44] V3A,[45] and V6.[46]

Experimental Protocol for the MOT During Pretraining and Post-training Tests

To evaluate whether our PL protocol generalizes to other motion-based visual tasks, we conducted additional experiments using a MOT task in five MD patients and four controls (CTRL6 did not perform the task). Participants completed two sessions, each lasting approximately 1 hour, before and after training. These sessions were conducted independent of the pretests and post-tests. Our limited number of participants here is owing to the fact that several patients were unable to take part in these additional measurements, considering the already lengthy duration of the training and other tests. MOT is a high-level cognitive task designed to assess how individuals can divide their spatial attention to track multiple objects over time (see, for example, Sears & Pylyshyn [2000][47]). Visual stimuli were created using MATLAB (R2021b) with the Psychophysics Toolbox and were projected onto a large convex screen (56 × 40 degrees of visual angle, 60 Hz refresh rate, 1024 × 768 resolution) in a dark room at a viewing distance of 180 cm. The design of the stimuli was adapted from a previous study on MOT.[48] The display consisted of either six or eight black disks, each with a diameter of 6.4 degrees of visual angle, moving on a white background (Fig. 2D). A frame of 6 degrees of visual angle was added at the edges of the screen. At the start of each trial, disks were randomly placed on the screen without overlapping. One-half of the disks were randomly designated as targets and flickered for 2 seconds, and the remaining disks, designated as distractors, remained unchanged. After this identification period, all disks moved for 10 seconds in random

directions at a constant velocity of either 12 or 16 degrees of visual angle per second, depending on whether the number of targets was three or four, respectively. When disks collided, their trajectories were reassigned to be opposite and collinear to the line passing through their centers. At the end of each trial, one disk was highlighted, and participants had to report whether it was a target. Given the proportion of targets, the chance level was 50% in both conditions. In control participants, the MOT task relied on a gaze-contingent paradigm in which an artificial scotoma was continuously centered on gaze fixation. Eye movements were recorded using an EyeLink 1000 eye-tracker (sampling rate, 1 kHz) positioned 30 cm in front of the participant. As in previous experiments, each control participant was assigned an artificial scotoma matching the surface area of that of their corresponding patient. However, in the present study the scotoma was rendered in the same color as the background (white). A known limitation of gaze-contingent paradigms occurs during blinks (Aguilar & Castet, 2011).[49] As the upper eyelid begins to close, the eye tracker detects an apparent downward shift in the pupil center, causing the scotoma to transiently shift downward before disappearing entirely as the blink progresses. To mitigate this artifact, blinks were detected using a threshold on pupil size. During detected blinks, the artificial scotoma was held at the last valid gaze position. This procedure prevented the illusory downward displacement during blinks and ensured that the scotoma remained visible at the correct location. Note that, because MD patients performed the task using their natural scotoma, a gaze-contingent paradigm was not applicable in this population. All recordings in MD patients and controls were conducted monocularly.

Additional Measures During Pretraining and Post-training Tests

During the pretraining and post-training test, patients also completed the BDI-II and the National Eye Institute's VFQ-25 once again. We also reassessed the visual acuity of all participants (patients and controls) using the Freiburg Visual Acuity Test (see Participants). These additional measurements enabled us to assess whether the training enhanced scores on these metrics and to ensure that their vision did not significantly decline owing to their condition during the protocol.

Statistical Analyses

For each participant, we averaged the motion discrimination thresholds, the PSCs, and the spatial extent of activation across runs. The effects of PL were assessed using aligned-ranks transformation (ART) ANOVA,[50] with the training session (pre or post) as the within-subject factor and the group (patient or control) as the between-subject factor. These nonparametric tests were performed using the ARTool package in R. To complete our analyses, we calculated the Cohen's dz corresponding with the changes in behavioral (or fMRI) measurements after training in each group.

Data and Code Availability

All the data associated with the PL experiments are provided at the following link: https://osf.io/jx9cd/overview?view_only=88ad20324b59437ba2bfbfb1cd2c3961 MRI and fMRI data are available upon request at the following email address: promoteur.cpp@cerco.cnrs.fr. These data have undergone spatial normalization, in compliance with the General Data Protection Regulation under which this project is carried out.

Results

Eleven patients (age range, 25–81 years; seven males, four females), diagnosed with either AMD or STG (Table 1), participated in this study. Each patient and their corresponding control underwent two sessions of pretest and post-test psychophysical measurements. Additionally, they completed 12 sessions of PL distributed over 4 weeks (Figs. 2A, 2B). After training, post-test measurements were conducted within 2 weeks.

In addition to these measurements, a subset of 18 participants (9 MD patients and their controls) also underwent fMRI recordings (Fig. 2C) and 9 participants (5 MD patients and 4 controls) performed the MOT task (Fig. 2D).

PL Learning Effects on Motion Perception

We measured motion direction discrimination thresholds in 11 MD patients and their age- and gender-matched controls before and after a PL protocol that included 12 sessions lasting approximately 1 hour. In control participants, the central part of the visual field was masked using an artificial scotoma of the same dimensions as in their paired patient to equalize visual inputs. Thresholds obtained during the different tests in both groups are shown in color in Figures 3A and 3C. Direct comparisons between the pretraining and post-training thresholds measured in patients and controls are shown in Figures 3B and 3D, respectively. Participants whose performance improved following PL are positioned below the diagonal, in the lower right section of the panels. This visual representation allows for an immediate and intuitive identification of individual training effects, highlighting the proportion of participants who benefited from PL. Overall, we can observe that training diminished thresholds in both groups. The significance of this diminution was demonstrated using an ART ANOVA (see Methods) for which we found an effect of training ($P = 3 \times 10^{-5}$), but no difference between groups nor interactions ($P > 0.05$ in both cases). Specifically, average threshold values decreased from 65% to 47% in patients and from 67% to 40% in controls. This represents a reduction of approximately 20% to 25% across participants. The associated Cohen's dz were −0.86 and −1.41, suggesting moderately strong and very strong PL effect on coherence thresholds for patients and control participants, respectively. In summary, our findings demonstrate that PL can significantly enhance motion perception in both populations, despite their age and limited fields of view.

PL Learning Effects on Whole Brain Activations

Next, we characterize whether these improvements are associated with changes in brain activations. Note that the corresponding neuroimaging experiments were conducted in a subset of nine patients and their controls as MD7 and MD8 had contraindications to MRI. Figure 4 displays the lateral views of the inflated cortical surfaces of one representative MD patient (MD4, left) and his control (CTRL4, right).

Investigative Ophthalmology & Visual Science

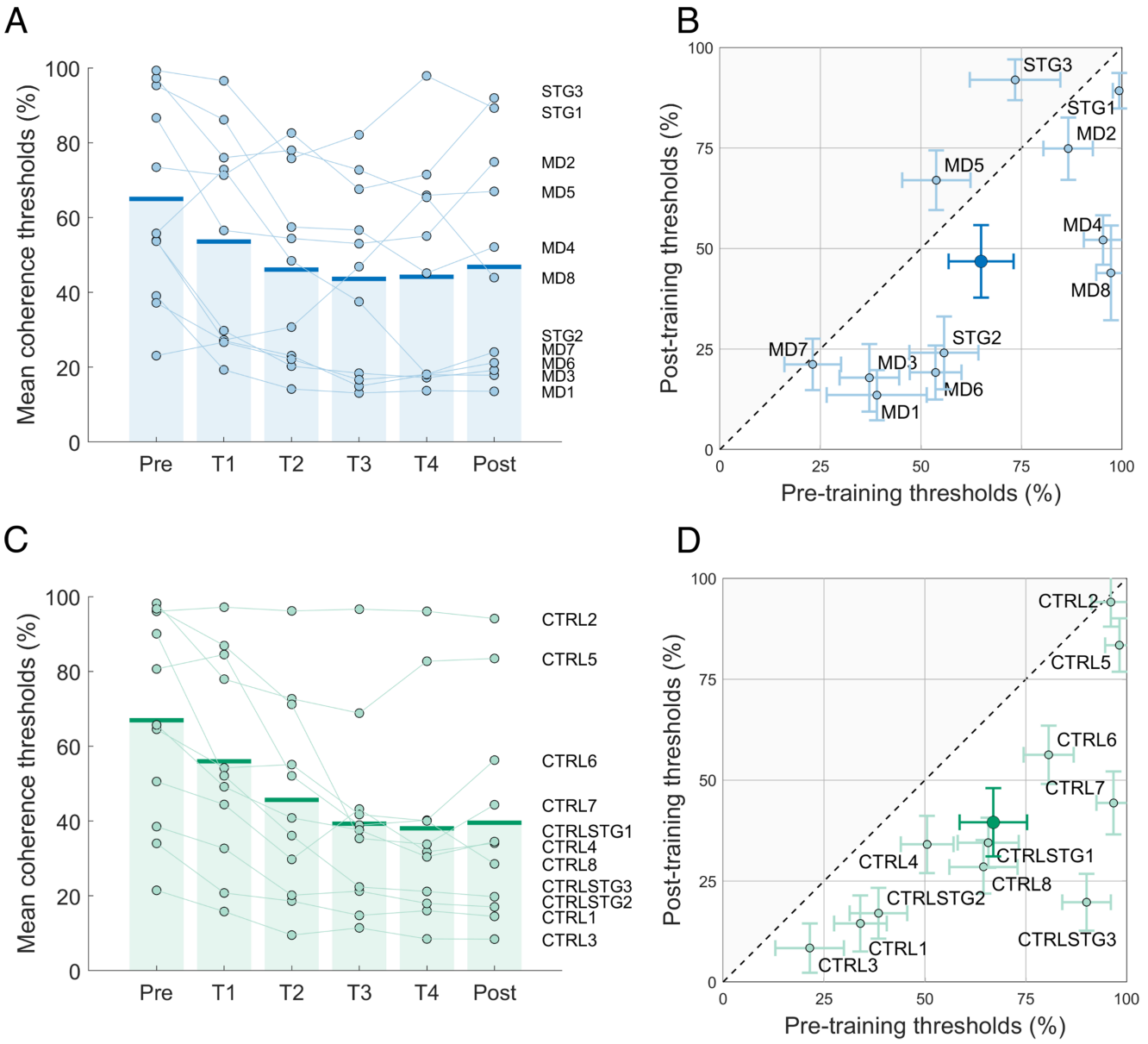

Figure 3. PL effects on motion perception. (**A**) Motion direction coherence thresholds measured in patients during the pretest, the four training sessions (T1–T4) and the post-test. The *thick lines* provide the average value across the population. Individual data are given by the *blue disks*. (**B**) Coherence thresholds measured during the post-training vs. pretraining sessions for each patient. The error bars provide the mean standard deviation estimated from the QUEST Bayesian adaptive approach. The *darker point* provides the average values across participants (the error bars give the associated standard errors of the mean). The data points located in the *shaded region* at the *top left* of the figure represent participants whose performance declined with training. (**C** and **D**) provide the same data as in (**A** and **B**) for control participants.

Pretraining and post-training activations (t-score, $P < 0.001$, uncorrected) are respectively shown in the upper and lower rows. Cortical nodes with strongest responses to translational motion compared with static dots appear in hot colors (yellow to red), whereas nodes with stronger responses to the opposite contrast are represented in cold colors (light blue to dark blue). The equivalent activations for the other participants are displayed in Figure 5. The medial views of these activations are shown in Supplementary Figure S1 for all participants.

As detailed in a previous study by our group,[36] both patients and controls exhibited significantly stronger responses to motion stimuli before training within a cortical network that includes areas hMT+, V3A, and V6 (refer to the captions of Figs. 3 and 4 for more details on their anatomical locations), as well as portions of early visual areas (V1, V2, and V3) that process peripheral vision (Supplementary Fig. S1). Interestingly, motion-selective responses after training appear very similar to those observed before training in both populations, with significant activations in the same set of areas (for comparison, Talairach coordinates of areas hMT+, V3A, and V6 measured before and after training are provided in Supplementary Table S1). We did not observe the emergence of activations in additional

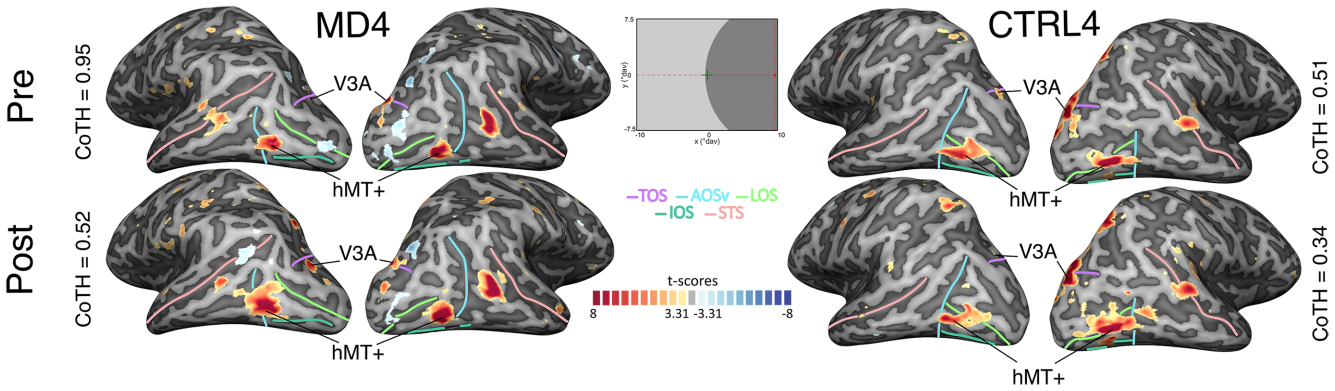

Figure 4. Comparison between BOLD responses to the translational motion condition and to its control condition (static dots) in one representative patient (MD4) and his age- and gender-matched control (CTRL4) before (*upper row*) and after (*upper row*) PL. Activations are shown on inflated individual cortical surfaces. Gyri appear in *pale gray* and sulci are shown in *darker gray*. Cortical nodes with significantly stronger responses to translational motion appear in *yellow/red* and nodes with significantly stronger responses to static dots are shown in *blue*. Data were thresholded at a P value of $<10^{-3}$ (uncorrected). Colored lines provide the anatomical positions of the inferior occipital sulcus (IOS, in *olive green*), of the lateral occipital sulcus (LOS, *in green*), of the transverse occipital sulcus (TOS, *in purple*), of the ventral part of the anterior occipital sulcus (AOSv, *in cyan*), and of the superior temporal sulcus (STS, *in red*). Significant activations can notably be observed in areas hMT+ (within or posterior to the AOSv, in between the IOS and the LOS) and V3A (within the TOS). The *central panel* illustrates the visual stimulation used during the experiment. During fMRI recordings, MD4 fixed the center of the screen (*green cross*) using his PRL, while CTRL4 gazed rightward at the position of MD4's fovea (*red cross*). The *dark region* represents the artificial scotoma (see Fig. 1 for more details on its definition). *Dotted lines*, not shown during the recordings, indicate the positions of the horizontal and vertical meridians. Additionally, coherence thresholds (CoTH) estimated through psychophysical measurements are provided.

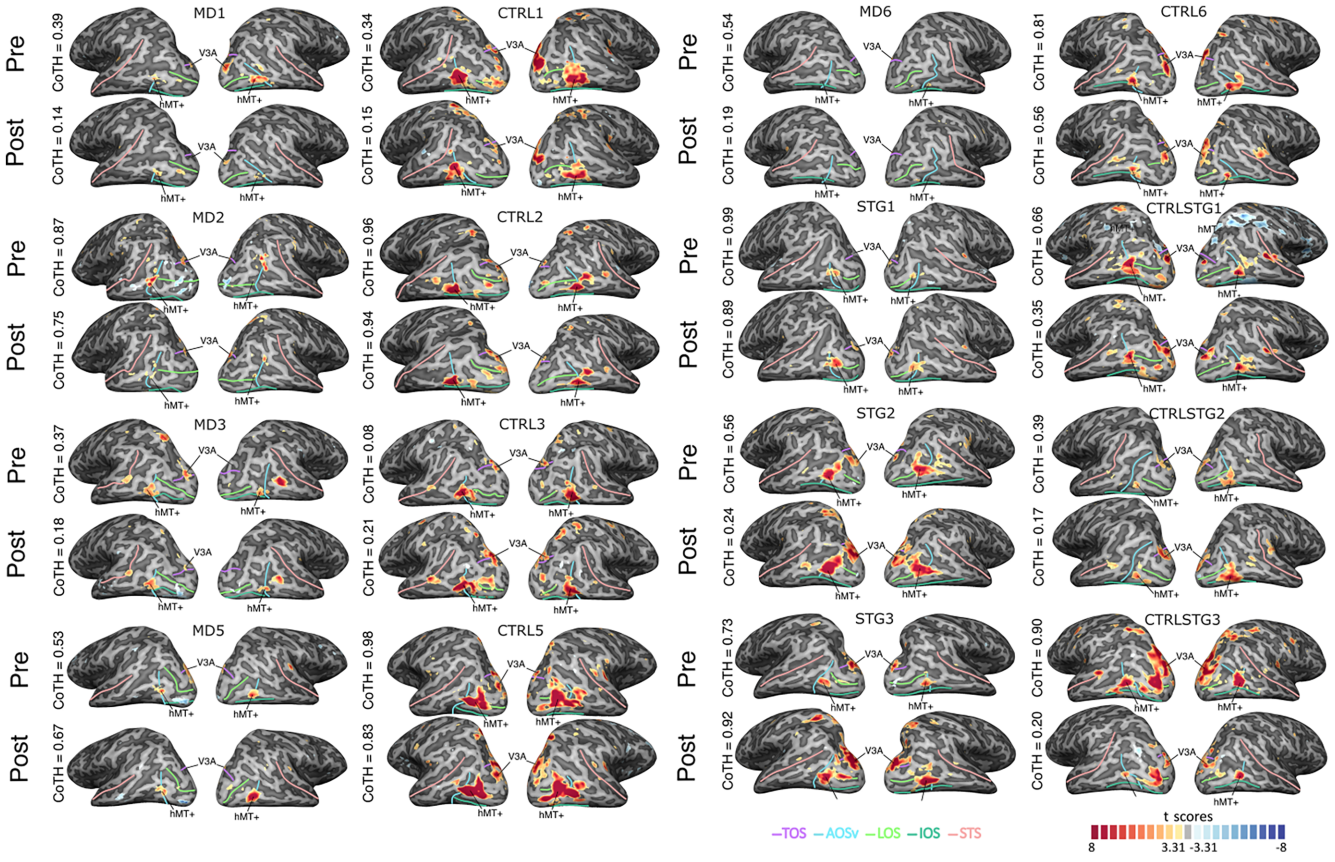

Figure 5. Comparison between BOLD responses to the translational motion condition and to its control condition (*static dots*) before (*upper rows*) and after (*lower rows*) training in all participants, except MD4 and his control (CTRL4), whose data are provided on enlarged views in Figure 4. Significantly stronger responses to motion are shown on lateral views of the cortical surfaces for MD patients (*left*) and their controls (*right*). See Figure 4 for the details of the legend.

Investigative Ophthalmology & Visual Science

Table 2. Dice Indexes and Correlation Scores Obtained for the Comparison Between PreTraining and Post-training Activations Measured in MD Patients and Their Controls

		Correlation				Correlation	
Patient	**Dice Index**	**Rho**	***P* Value**	**Controls**	**Dice Index**	**Rho**	***P* Value**
MD1	0.316	0.35	$<10^{-10}$	CTRL1	0.726	0.62	$<10^{-10}$
MD2	0.142	0.07	$<10^{-10}$	CTRL2	0.596	0.52	$<10^{-10}$
MD3	0.511	0.45	$<10^{-10}$	CTRL3	0.517	0.47	$<10^{-10}$
MD4	0.54	0.44	$<10^{-10}$	CTRL4	0.822	0.61	$<10^{-10}$
MD5	0.612	0.53	$<10^{-10}$	CTRL5	0.634	0.48	$<10^{-10}$
MD6	0.185	0.17	$<10^{-10}$	CTRL6	0.631	0.51	$<10^{-10}$
STG1	0.367	0.29	$<10^{-10}$	CTRLSTG1	0.428	0.29	$<10^{-10}$
STG2	0.583	0.44	$<10^{-10}$	CTRLSTG2	0.547	0.51	$<10^{-10}$
STG3	0.461	0.41	$<10^{-10}$	CTRLSTG3	0.547	0.39	$<10^{-10}$
Mean	0.407	0.343		Mean	0.613	0.501	

brain areas following PL. Before delving further into the effects of training within motion-selective areas (detailed in PL Learning Effects on Responses Within Motion Selective Areas), we present the results of correlation analyses between the pretraining and post-training activations, which were highly significant (Table 2). The substantial overlap between these activations was further demonstrated using Dice coefficients.[51] These coefficients ranged from 0.14 to 0.61 in patients (average, 0.40) and from 0.43 to 0.82 in controls (average, 0.61). Although these values are slightly lower in MD patients, possibly owing to generally worse signal-to-noise ratios in this population, they indicate a high correspondence between the pretraining and post-training activations.[52–55] Overall, these results demonstrate the high reproducibility of our measurements within individual participants across recording sessions and suggest that PL does not induce large-scale changes in brain responses. We did not perform whole brain group-level analyses of post-training vs. pretraining activations owing to substantial variability in scotoma properties and PRL positions among our MD patients. This variability leads to differences in visual input and associated cortical activations, making it difficult to obtain reliable results when fMRI responses across patients (or controls) are projected onto a common brain template.

PL Learning Effects on Responses Within Motion Selective Areas

Next, we examined the impact of training on activations at a finer spatial scale within motion-selective areas. To avoid circular analyses, we calculated the differences in percentages of signal changes (PSCs) before and after PL within independently defined ROIs. These ROIs were centered on the Talairach coordinates reported in the literature for hMT+,[44] V3A,[45] and V6.[46] We were particularly interested in effects within the hMT+ ROI, because previous studies have demonstrated that this area retains a degree of plasticity after central vision loss. The differences in PSC obtained before and after training are illustrated in Figure 6. For hMT+, it is evident that activations increased post-training compared with pretraining in both patients and controls, as indicated by the data points lying in the upper left part of the diagrams. This observation was statistically confirmed using an ART ANOVA, which revealed a significant effect of training on PSC differences in hMT+ ($P = 0.002$). The associated Cohen's dz were 1.00 in MD patients and 0.56 in controls, suggesting a strong effect of PL on hMT+ in the first group and a moderate effect in the latter. The same ART ANOVA did not show any significant differences between groups ($P = 0.066$) or any significant interactions between training and groups ($P = 0.279$). When applied to V3A and V6, this analysis did not uncover any significant effects in these ROIs. In addition to examining increases in activation, we also assessed whether training modifies the spatial extent of activation in the three ROIs. We did not find any significant effect of PL in this case (Supplementary Fig. S2). However, we observed a moderate group effect in area hMT+, suggesting that activation in this ROI is generally more extended in controls ($P = 0.047$). In our previous study on motion processing in MD patients,[36] this effect was not observed ($P = 0.11$), but that analysis was based on only 14 participants (7 MD patients and their controls), compared with 18 in the present study.

We show here the results of the fMRI analyses conducted using ROIs with a 10 mm radius. Similar effects were observed with radii of 5 mm and 15 mm (see Supplementary Fig. S3).

We also investigated whether the increase in activations observed in hMT+ after PL in both patients and controls correlated with reductions in motion discrimination thresholds. However, no significant effects were found (Supplementary Fig. S4). Similar analyses in areas V3A and V6 also revealed no significant correlations between BOLD responses and behavioral performance.

Generalization of PL on Another Task, on Visual Acuity, and on the National Eye Institute's VFQ-25

Finally, we tested whether PL can also generalize to another motion task based on higher-level cognitive mechanisms and notably spatial attention: MOT in a subset of participants (four MD patients and their respective controls). Two additional sessions lasting approximately 1 hour were performed before and after training, independent from the pretests and post-tests. Participants had to track target disks among visually identical distractors for 10 seconds. We used two conditions which differed in the number of targets and distractors (either three among six or four among eight). Results before and after PL are shown in Figure 7.

On average, we can observe that both patients and controls improved their performance after learning with detection scores that went from 77.6% to 83.9% across the two tasks (Figs. 7A, 7D). The significance of this performance

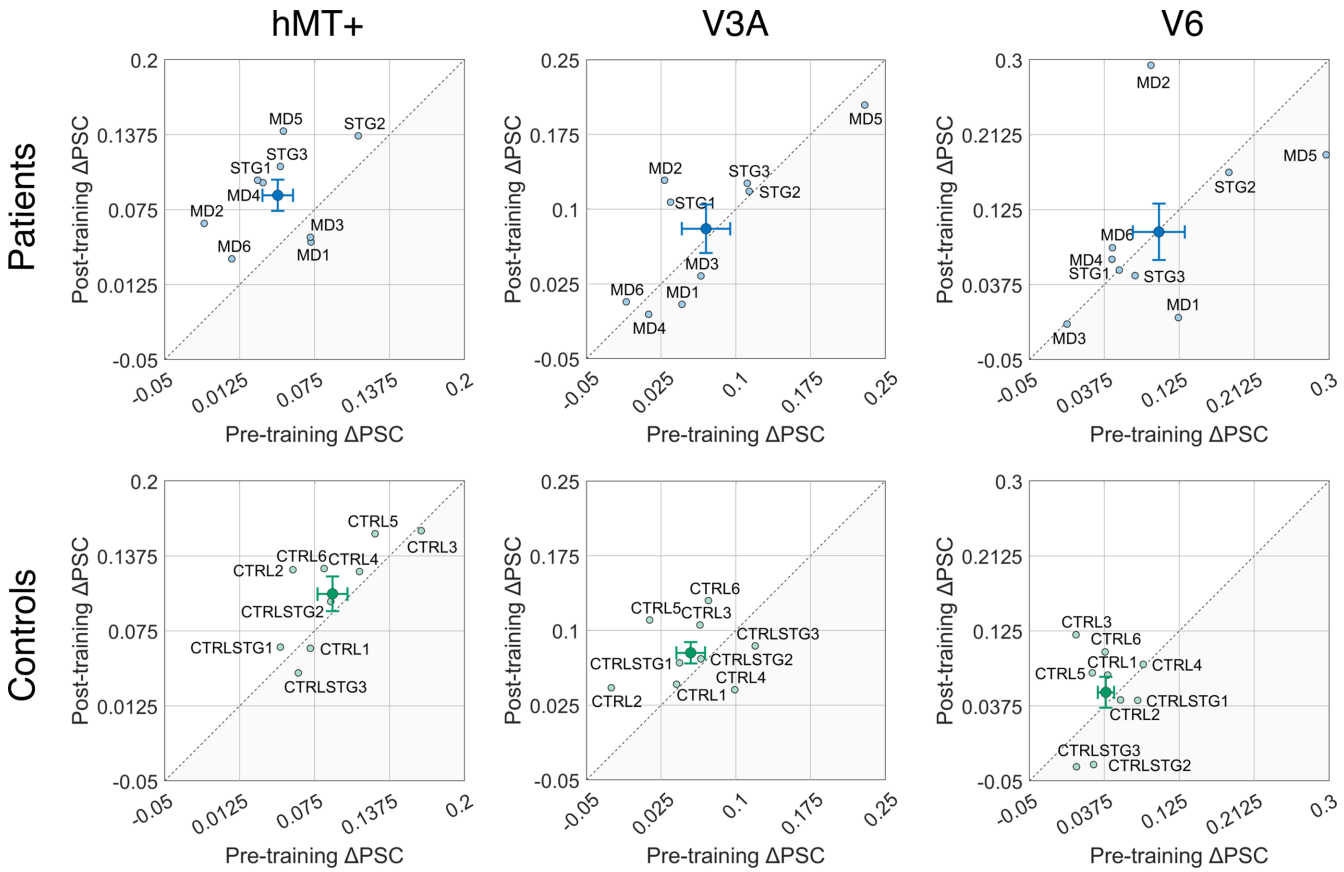

Figure 6. PL effects on brain activations. The percentage of signal changes measured during the post-training vs. pretraining sessions in each patient (*higher panels*) and control participants (*lower panels*) in hMT+ (*left column*), V3A (*middle column*), and V6 (*right column*) ROIs. The *darker points* provide the average values across participants (the error bars give the associated standard errors of the mean). The data points located in the *shaded region* at the *lower right* of the figure represent participants whose PSCs declined with training.

enhancement was confirmed using an ART ANOVA, which revealed an effect of training ($P = 0.004$), but no differences between groups or second-order interactions ($P > 0.05$ in both cases). The associated Cohen's dz were 1.78 in MD patients and 1.39 in controls, suggesting a very strong effect of PL on detection scores in both groups. Performance improvements were also observed when examining each condition separately (Figs. 7B and 7E for the first condition, and Figs. 7C and 7F for the second condition, respectively). Overall, these results suggest that our protocol enhanced MOT, even though the MOT task was not included in the training sessions. Future studies from our group will aim to confirm these findings with a larger participant sample.

To complete these analyses, we examined whether the performance improvements in the MOT task were correlated with the reduction of motion discrimination thresholds or changes in fMRI responses in motion-selective areas. However, we did not observe any significant effects (Supplementary Fig. S4).

Next, we evaluated whether the training affected patients' visual function, depressive symptoms, and visual acuity (see Additional Measures). Visual function was assessed using the 25-item National Eye Institute VFQ-25, which covers 12 categories (such as near activities, distance activities, mental health, dependency, and peripheral vision), each with 1 to 4 items. As an example, the dependency category included three questions, each scored from 0 to 100 in increments of 25, with the average value forming the category score. Depressive symptoms were assessed using the BDI-II, consisting of 21 questions scored 0 to 3 (from not at all to all the time). Total scores range from 0 to 63, and only participants with scores of less than 19, indicating no depressive symptoms, were included (see Methods). We found no significant effects of the training on visual acuity (this was also verified for control participants). However, PL induced a significant decrease in the BDI-II score, as well as a significant increase in the dependency factor score of the NEI-VFQ-25 (Supplementary Fig. S5A), indicating that patients reported feeling more independent after the training. Other factors, such as general vision perception and sociability, remained stable over time. For transparency, the improvement scores for all factors are reported in Supplementary Table S2. Finally, we examined whether any of these scores correlated with behavioral performance or BOLD responses in our ROIs. A significant correlation was found only between BDI scores and the pretest PSC difference in both hMT+ and V3A (Spearman correlation, $P = 0.025$ and $P = 0.009$, respectively).

As a final verification, because one pair of participants was significantly younger than the others (STG3/CTRLSTG3, approximately 25 years old), we confirmed that their data did not influence our results. We replicated the statistical analysis, both behavioral and functional, on the remaining participants and arrived at the same conclusions. The coher-

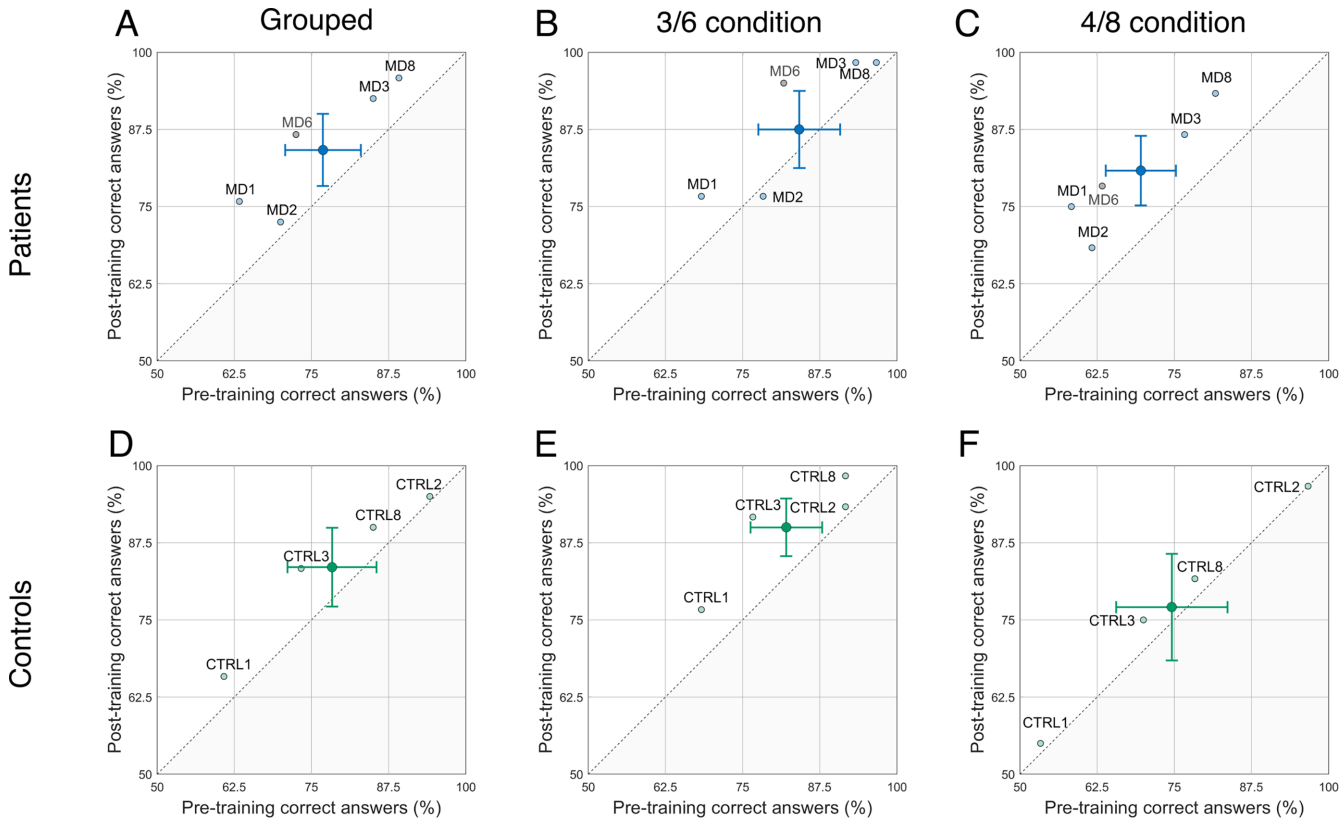

Figure 7. PL effects on the MOT task. (**A**) Average percentages of correct detections across the two experimental conditions during the post-training vs. pretraining sessions for each patient. Performance for the first (detecting three targets across six disks) and second (detecting four targets across eight disks) conditions are respectively shown in (**B** and **C**). The *darker points* provide the average values across participants (the error bars give the associated standard errors of the mean). The data points located in the shaded region at the lower right of the figure represent participants whose performance declined with training. The corresponding results for control participants are provided in (**D**, **E**, and **F**, respectively). Data collected from MD6, for whom their control did not participate, is presented here for completeness.

ence thresholds remained significantly lower post-training ($P = 3.3 \times 10^{-6}$), and the activations measured in hMT+ were also stronger ($P = 0.005$).

Discussion

Currently, there is no known cure for MD,[56] underscoring the importance of developing rehabilitation strategies that can maintain or even improve patients' visual perception in everyday tasks. Our study aligns with this research direction, aiming to ascertain whether PL can enhance motion processing in patients with MD, despite their loss of central vision. Motion perception plays a fundamental role in how we interact with and navigate through our environment. It notably permits us to detect and track moving objects or individuals in the surroundings[22] or to integrate our path during movements.[21] Here, we conducted training with 11 patients who were affected by either AMD or STG with dense bilateral scotoma, as well as 11 control participants matched for age and gender, using a motion direction discrimination task. To ensure comparable visual inputs between the two groups, central vision in control participants was masked using an artificial scotoma of the same size as that of their paired patients. Our findings revealed that training significantly improved discrimination thresholds, reducing them by more than 20% in both populations (Fig. 3). Additionally, these behavioral improvements were linked to increased activation in the hMT+ area. Furthermore, a subset of patients also showed enhanced performance on a MOT task that was not part of the training.

Numerous studies in cognitive sciences and neuropsychology have applied PL to dynamic visual tasks and demonstrated its potential to enhance motion perception in both young individuals,[7,57,58] older adults with normal vision,[27] and patients with lesions in early visual cortex.[59] Our findings align with these studies; we observed that PL significantly improved motion direction discrimination in our participants, reducing thresholds by more than 20%. Specifically, thresholds decreased from 65% to 47% in MD patients and from 67% to 40% in control participants; however, no statistical group difference has been found. Importantly, these improvements were achieved without reliance on central vision, illustrating that neural plasticity remains effective in this context. Although previous research has shown that PL can enhance visual perception in MD patients[12,60] (see Maniglia et al. [2016][5] for a review), our study is the first to demonstrate this effect in the context of a motion task. Including both a patient and a control group was motivated by the expectation that peripheral vision processing may differ across these populations, as recent evidence suggests that motion-selective areas can reorganize after central vision loss.[29,31] Such reorganization could potentially impact, either positively or negatively, the effectiveness of PL. For this reason, directly comparing training-

related improvements between patients and healthy participants was essential. Although PL effects were similar across groups in the present study, this outcome could not have been assumed before the experiment. The absence of group differences, therefore, supports that PL in motion perception remains robust despite long-term central vision loss.

To date, only one study has investigated the neural correlates of PL in patients with maculopathy.[16] In this study, patients and age-matched controls without an artificial scotoma underwent a 3-week training program (six sessions lasting approximately 1 hour each) to perform a texture discrimination task. Significant behavioral improvements were observed after the training, but these were accompanied by only modest and nonsignificant modifications in BOLD responses in the early visual cortex. Another study by the same group found similar effects in patients with MD who were trained over 6 months to improve their ocular fixation stability.[17] In this case, changes in brain activation correlated with improvements in fixation stability. However, these correlations were observed only during the initial phase of training and for specific stimuli (images), but not for others (checkerboards). Because these effects were observed across most of the explored visual areas (V1, V2, and V3, as well as in the fusiform gyrus and the lateral occipital lobe), it is possible that they reflect an improvement in attention allocation rather than a genuine modification of neural selectivity. In our study, we found a significant increase in BOLD responses in one functional area (hMT+), but not in others. Whole-brain activations before and after training were very similar, suggesting that only responses in the hMT+ area were modified. The hMT+ area is highly selective for motion (see, e.g., Tootell et al. [1995][61]), causally involved in motion perception,[62,63] and PL has been shown to modulate its activity in young adult participants[25] (see also Larcombe et al. [2018][64] for effects within its hMST subregion), possibly through a sharpening of its underlying neural units.[65] Here, we show for the first time that these effects are still observable in older adults with normal vision (even when their central vision is masked) and in patients with MD. The plasticity mechanisms observed in this area are not entirely surprising, as a recent neuroimaging study found that functional connectivity between the portions of early visual areas (V1, V2, and V3) that respond to peripheral vision and hMT+ was reinforced in individuals with central vision loss.[32] In animal models, activation enhancements in areas homologous to hMT+ were also reported following central vision loss (see Burnat et al. [2017][29] and Shao et al. [2013][31] for effects in the cat posteromedial lateral suprasylvian area and in macaque area MT, respectively). Importantly, our fMRI and psychophysical recordings were conducted separately, which may explain the lack of a significant correlation between BOLD responses, particularly in area hMT+, and behavioral performance. During the neuroimaging sessions, participants reported infrequent targets at fixation while visual stimuli alternated between fully coherent motion (100%) in the upward or downward direction and static dots. This fMRI design was chosen to maximize the signal-to-noise ratio of the data, because we anticipated that older participants would be more prone to movement during scanning, thereby increasing the risk of motion-related artifacts. Future PL studies in MD patients could incorporate a concurrent psychophysical task during fMRI to more directly investigate how PL influences motion-selective areas such as hMT+ or V3A[66] and modulates neural responses in higher-level, decision-related regions that integrate information from these areas.[67]

One limitation of PL is that the improvements observed are often specific to the stimuli used during training. Typically, performance enhancements are evident only when the testing conditions closely mirror those of the training. This includes factors such as the motion direction of the stimuli,[7,57] spatial frequency,[68] orientation,[69,70] or the retinal location of stimulation.[18] However, several studies challenged this notion of specificity, suggesting that the benefits of PL may extend beyond the trained tasks. For example, Barollo et al. (2017)[71] demonstrated that training on a lateral masking paradigm could enhance performance in a foveal crowding task and improve visual acuity in patients. McGovern et al. (2012)[72] also reported that participants trained on orientation discrimination showed improvements in a curvature task and, to a lesser extent, in a global form task. This finding suggests a potential transfer of learning from low-level to higher-level brain areas, contingent on overlapping computations between the tasks. The complexity of the training and test tasks is also a contributing factor to transfer. Training on easy tasks (such as discriminating between two widely separated directions of motion) is believed to be more likely to transfer than training on difficult tasks (e.g., discriminating between two similar directions of motion), because it relies on more broadly tuned neural populations (Ahissar & Hochstein, [2004][73]; see, however, Liu & Weinshall [1998][74] for evidence that learning on difficult tasks can still transfer via an improved learning rate). In our study, we found that PL on a relatively low-level motion direction discrimination task also improved the capacity to track multiple objects over time (MOT) in a subset of participants (five patients and four controls) (Fig. 7). MOT is a complex task that involves the dynamic allocation of spatial attention and is believed to reflect cognitive processes in real-world situations, such as driving or navigation. This makes it particularly important for patients with MD.[75] MOT activates an extensive cortical network that includes area hMT+ for early motion processing and higher-level areas in the parietal and frontal cortices, which are involved in the dynamic allocation of spatial attention.[76] Although our MOT task was only performed on a limited number of participants (principally because for several participants, it was difficult to further extend the already long duration of our experimental protocol), we observed a significant improvement in performance during the post-training tests in both populations. This enhancement may stem from modifications in neural processing within the hMT+ region and, consequently, further along the motion processing pathway (e.g., in the frontal eye field). It could, therefore, reflect a transfer from low-level to higher-level brain areas that exploit common motion computations in the two tasks (as observed by McGovern et al. [2012],[72] for orientation and curvature discrimination). In our case, transfer may have been facilitated by the fact that participants discriminated between two opposite motion directions (upward vs. downward), which can be considered an easy task, even though dot coherence was adjusted online to maintain a constant level of performance. Further investigation is needed to isolate the real impact of the training on these improvements. Although this issue was not addressed in our study, future research could include a control group that completes only the pretests and post-tests without undergoing the training. Nevertheless, our results suggest that the benefits of PL on motion direction discrimination can transfer to more complex and

ecologically valid tasks. This transfer effect highlights the potential of PL as a tool for enhancing cognitive functions in both healthy individuals and those with visual impairments. Further research is needed to explore the underlying neural mechanisms and to optimize training protocols for maximizing transfer effects in real-world applications, possibly through brain stimulation techniques, such as transcranial current stimulation (see, e.g., Contemori et al. [2024][77]).

A limitation of our study is the relatively small sample size, which consisted of 11 patients with MD and their respective controls. Recruiting MD patients for extensive PL protocols, such as the 12 sessions conducted in our study, combined with neuroimaging experiments, presents significant challenges. Our sample size can be attributed to our stringent inclusion criteria. We exclusively enrolled patients without long-term illnesses, who had stable PRL in at least one eye, exhibited typical cognitive function and psychological states, and had no contraindications for fMRI recordings. Despite these constraints, our study aligns with previous research involving maculopathy patients[16,17] and led to significant and reliable effects of training. Overall, our patients completed approximately 4 hours of training across the 12 sessions, each lasting approximately 20 minutes. Considering the improvements observed in the motion discrimination task (approximately 20%–25%) and the potential generalization to other motion-based tasks, we believe that our approach holds clear promise as a therapeutic intervention for MD patients. However, several controls are needed before considering practical applications. Given that the frequency and duration of current care protocols provided by health professionals vary widely between centers (see, e.g., Binns et al. [2012][78]; Raphanel et al. [2018][79]), it is important to test whether the effects of our PL protocol can be achieved with sessions distributed over longer periods, potentially with variable intervals. To better accommodate the limited mobility of MD patients, training at home could be an interesting alternative, although it remains to be verified whether comparable effects can be obtained under a less controlled protocol. Finally, it is also crucial to assess the longevity of the training effects, particularly whether they persist over several months. These questions represent several avenues that our group plans to investigate in the near future.

Acknowledgments

The authors thank Victor Vattier for his involvement in the pilot recordings of the MOT task. Our thanks also go to Pauline Meyer for her assistance with the OCT exams, and to Judith Eck for her valuable advice on fMRI analysis. Additionally, we are grateful to Ilia Korjoukov and Louise Kauffmann for their contributions to the development of our MRI paradigm.

Supported by a French grant from the Agence Nationale de la Recherche (ANR-21-CE28-0021, ANR PRC ReViS-MD; awarded to CP and BRC).

This work was performed on the Inserm/UPS UMR1214 Technical Platform of Toulouse and the IRMaGe platform member of France Life Imaging network (grant ANR-11-INBS-0006) for Grenoble.

Disclosure: **C. Michaud**, None; **C. Faurite**, None; **J. Guénot**, None; **M. Gallice**, None; **C. Chiquet**, None; **N. Vayssière**, None; **I. Berry**, None; **Y. Trotter**, None; **R. Baurès**, None; **M. Rosito**, None; **V. Soler**, None; **C. Peyrin**, None; **B.R. Cottereau**, None

References

1. Wong WL, Su X, Li X, et al. Global prevalence of age-related macular degeneration and disease burden projection for 2020 and 2040: a systematic review and meta-analysis. *Lancet Glob Health*. 2014;2(2):e106–116.
2. Hassan SE, Lovie-Kitchin JE, Woods ARL. Vision and mobility performance of subjects with age-related macular degeneration. *Optom Vis Sci*. 2002;79(11):697–707.
3. Wood JM, Lacherez PF, Black AA, Cole MH, Boon MY, Kerr GK. Postural stability and gait among older adults with age-related maculopathy. *Invest Ophthalmol Vis Sci*. 2009;50(1):482.
4. Goldstone RL. Perceptual learning. *Annu Rev Psychol*. 1998;49:585–612. doi:10.1146/annurev.psych.49.1.585.
5. Maniglia M, Cottereau BR, Soler V, Trotter Y. Rehabilitation approaches in macular degeneration patients. *Front Syst Neurosci*. 2016;10:107.
6. Andersen GJ, Ni R, Bower JD, Watanabe T. Perceptual learning, aging, and improved visual performance in early stages of visual processing. *J Vis*. 2010;10(13):4.
7. Ball K, Sekuler R. Direction-specific improvement in motion discrimination. *Vision Res*. 1987;27(6):953–965.
8. DeLoss DJ, Watanabe T, Andersen GJ. Optimization of perceptual learning: effects of task difficulty and external noise in older adults. *Vision Res*. 2014;99:37–45.
9. Deveau J, Seitz AR. Applying perceptual learning to achieve practical changes in vision. *Front Psychol*. 2014;5:1166.
10. Levi DM, Li RW. Perceptual learning as a potential treatment for amblyopia: a mini-review. *Vision Res*. 2009;49(21):2535–2549.
11. Chacón-López H, Pelayo FJ, MD L-J, et al. Visual training and emotional state of people with retinitis pigmentosa. *J Rehabil Res Dev*. 2013;50(8):1157–1168.
12. Chung ST. Improving reading speed for people with central vision loss through perceptual learning. *Invest Ophthalmol Vis Sci*. 2011;52(2):1164–1170.
13. Tarita-Nistor L, Brent MH, Steinbach MJ, Markowitz SN, González EG. Reading training with threshold stimuli in people with central vision loss: a feasibility study. *Optom Vis Sci*. 2014;91(1):86.
14. Maniglia M, Pavan A, Sato G, et al. Perceptual learning leads to long lasting visual improvement in patients with central vision loss. *Restor Neurol Neurosci*. 2016;34(5):697–720.
15. Maniglia M, Soler V, Cottereau B, Trotter Y. Spontaneous and training-induced cortical plasticity in MD patients: hints from lateral masking. *Sci Rep*. 2018;8(1):90.
16. Plank T, Rosengarth K, Schmalhofer C, Goldhacker M, Brandl-Rühle S, Greenlee MW. Perceptual learning in patients with macular degeneration. *Front Psychol*. 2014;5:1189.
17. Rosengarth K, Keck I, Brandl-Rühle S, et al. Functional and structural brain modifications induced by oculomotor training in patients with age-related macular degeneration. *Front Psychol*. 2013;4:428.
18. Karni A, Sagi D. Where practice makes perfect in texture discrimination: evidence for primary visual cortex plasticity. *Proc Natl Acad Sci USA*. 1991;88(11):4966–4970.
19. Smirnakis SM, Brewer AA, Schmid MC, et al. Lack of long-term cortical reorganization after macaque retinal lesions. *Nature*. 2005;435(7040):300–307.
20. Baseler HA, Gouws A, Haak KV, et al. Large-scale remapping of visual cortex is absent in adult humans with macular degeneration. *Nat Neurosci*. 2011;14(5):649–655.
21. Kearns MJ, Warren WH, Duchon AP, Tarr M. Path integration from optic flow and body senses in a homing task. *Perception*. 2002;31(3):349–374.

Investigative Ophthalmology & Visual Science

22. Warren PA, Rushton SK. Optic flow processing for the assessment of object movement during ego movement. *Curr Biol*. 2009;19(18):1555–1560.
23. Mar RA, Kelley WM, Heatherton TF, Macrae CN. Detecting agency from the biological motion of veridical *vs* animated agents. *Soc Cogn Affect Neurosci*. 2007;2(3):199–205.
24. Zohary E, Celebrini S, Britten KH, Newsome WT. Neuronal plasticity that underlies improvement in perceptual performance. *Science*. 1994;263(5151):1289–1292.
25. Vaina LM, Belliveau JW, des REB, Zeffiro TA. Neural systems underlying learning and representation of global motion. *Proc Natl Acad Sci U S A*. 1998;95(21):12657–12662.
26. Ball K, Sekuler R. Improving visual perception in older observers. *J Gerontol*. 1986;41(2):176–182.
27. Bower A. Aging, perceptual learning, and changes in efficiency of motion processing. *Vision Res*. 2012;61:144–156.
28. Eisen-Enosh A, Farah N, Polat U, Mandel Y. Perceptual learning based on a temporal stimulus enhances visual function in adult amblyopic subjects. *Sci Rep*. 2023;13(1):7643.
29. Burnat K, Hu TT, Kossut M, Eysel UT, Arckens L. Plasticity beyond V1: reinforcement of motion perception upon binocular central retinal lesions in adulthood. *J Neurosci*. 2017;37(37):8989–8999.
30. Villeneuve MY, Ptito M, Casanova C. Global motion integration in the postero-medial part of the lateral suprasylvian cortex in the cat. *Exp Brain Res*. 2006;172(4):485–497.
31. Shao Y, Keliris GA, Papanikolaou A, et al. Visual cortex organisation in a macaque monkey with macular degeneration. *Eur J Neurosci*. 2013;38(10):3456–3464.
32. Fleming LL, Defenderfer MK, Demirayak P, Stewart P, Decarlo DK, Visscher KM. Impact of deprivation and preferential usage on functional connectivity between early visual cortex and category-selective visual regions. *Hum Brain Mapp*. 2024;45(17):e70064.
33. Mangione CM, Lee PP, Gutierrez PR, et al. Development of the 25-item National Eye Institute Visual Function Questionnaire. *Arch Ophthalmol*. 2001;119(7):1050–1058.
34. Bach M. The Freiburg Visual Acuity Test-variability unchanged by post-hoc re-analysis. *Graefes Arch Clin Exp Ophthalmol*. 2007;245(7):965–971.
35. Guénot J, Trotter Y, Fricker P, Cherubini M, Soler V, Cottereau BR. Optic flow processing in patients with macular degeneration. *Invest Ophthalmol Vis Sci*. 2022;63(12):21.
36. Michaud C, Guénot J, Faurite C, et al. Motion processing in visual cortex of maculopathy patients. *J Neurosci*. 2025;45(30):e0283252025.
37. van Huet RAC, Bax NM, Westeneng-Van Haaften SC, et al. Foveal sparing in Stargardt disease. *Invest Ophthalmol Vis Sci*. 2014;55(11):7467–7478.
38. Graziano M, Andersen R, Snowden R. Tuning of MST neurons to spiral motions. *J Neurosci*. 1994;14(1):54–67.
39. Watson AB, Pelli DG. Quest: a Bayesian adaptive psychometric method. *Percept Psychophys*. 1983;33(2):113–120.
40. Goebel R, Esposito F, Formisano E. Analysis of functional image analysis contest (FIAC) data with brainvoyager QX: from single-subject to cortically aligned group general linear model analysis and self-organizing group independent component analysis. *Human Brain Mapp*. 2006;27(5):392–401.
41. Talairach J, Tournoux P. *Co-Planar Stereotaxic Atlas of the Human Brain: 3-Dimensional Proportional System: An Approach to Cerebral Imaging*. Stuttgart, Germany: G. Thieme; 1988..
42. Audurier P, Héjja-Brichard Y, De Castro V, et al. Symmetry processing in the macaque visual cortex. *Cerebral Cortex*. 2022;32(10):2277–2290.
43. Aedo-Jury F, Cottereau BR, Celebrini S, Séverac Cauquil A. Antero-posterior vs. lateral vestibular input processing in human visual cortex. *Front Integr Neurosci*. 2020;14:43. doi:10.3389/fnint.2020.00043.
44. Watson JDG, Myers R, Frackowiak RSJ, et al. Area V5 of the human brain: evidence from a combined study using positron emission tomography and magnetic resonance imaging. *Cereb Cortex*. 1993;3(2):79–94.
45. Tootell RBH, Mendola JD, Hadjikhani NK, et al. Functional analysis of V3A and related areas in human visual cortex. *J Neurosci*. 1997;17(18):7060–7078.
46. Pitzalis S, Sereno MI, Committeri G, et al. Human v6: the medial motion area. *Cereb Cortex*. 2010;20(2):411–424.
47. Sears CR, Pylyshyn ZW. Multiple object tracking and attentional processing. *Can J Exp Psycho*. 2000;54(1):1–14.
48. Pylyshyn ZW, Storm RW. Tracking multiple independent targets: evidence for a parallel tracking mechanism. *Spat Vis*. 1988;3(3):179–197.
49. Aguilar C, Castet E. Gaze-contingent simulation of retinopathy: some potential pitfalls and remedies. *Vis Res*. 2011;51(9):997–1012. doi:10.1016/j.visres.2011.02.010.
50. Wobbrock JO, Findlater L, Gergle D, Higgins JJ. The aligned rank transform for nonparametric factorial analyses using only ANOVA procedures. In: *Proceedings of the SIGCHI Conference on Human Factors in Computing Systems*. Vancouver, BC, Canada: ACM; May 7–12, 2011:143–146.
51. Dice LR. Measures of the amount of ecologic association between species. *Ecology*. 1945;26(3):297–302.
52. Gorgolewski KJ, Storkey AJ, Bastin ME, Whittle I, Pernet C. Single subject fMRI test–retest reliability metrics and confounding factors. *NeuroImage*. 2013;69:231–243.
53. Nettekoven C, Reck N, Goldbrunner R, Grefkes C, Weiß Lucas C. Short- and long-term reliability of language fMRI. *Neuroimage*. 2018;176:215–225.
54. Pajula J, Tohka J. How many is enough? Effect of sample size in inter-subject correlation analysis of fMRI. *Comput Intell Neurosci*. 2016;2016(1):2094601.
55. Wüthrich F, Lefebvre S, Nadesalingam N, et al. Test–retest reliability of a finger-tapping fMRI task in a healthy population. *Eur J Neurosci*. 2023;57(1):78–90.
56. Vyawahare H, Shinde P. Age-Related macular degeneration: epidemiology, pathophysiology, diagnosis, and treatment. *Cureus*. 2022;14(9):e29583. Published online September 26, 2022.
57. Ball K, Sekuler R. A specific and enduring improvement in visual motion discrimination. *Science*. 1982;218(4573):697–698.
58. Liu Z. Perceptual learning in motion discrimination that generalizes across motion directions. *Proc Natl Acad Sci USA*. 1999;96(24):14085–14087.
59. Huxlin KR, Martin T, Kelly K, et al. Perceptual relearning of complex visual motion after V1 damage in humans. *J Neurosci*. 2009;29(13):3981–3991.
60. Seiple W, Grant P, Szlyk JP. Reading rehabilitation of individuals with AMD: relative effectiveness of training approaches. *Invest Ophthalmol Vis Sci*. 2011;52(6):2938–2944.
61. Tootell R, Reppas J, Kwong K, et al. Functional analysis of human MT and related visual cortical areas using magnetic resonance imaging. *J Neurosci*. 1995;15(4):3215–3230.
62. Chakraborty A, Tran TT, Silva AE, Giaschi D, Thompson B. Continuous theta burst TMS of area MT+ impairs attentive motion tracking. *Eur J Neurosci*. 2021;54(9):7289–7300.
63. McKeefry DJ, Burton MP, Vakrou C, Barrett BT, Morland AB. Induced deficits in speed perception by transcranial magnetic stimulation of human cortical areas V5/MT+ and V3A. *J Neurosci*. 2008;28(27):6848–6857.
64. Larcombe SJ, Kennard C, Bridge H. Increase in MST activity correlates with visual motion learning: a functional

Investigative Ophthalmology & Visual Science

MRI study of perceptual learning. *Human Brain Mapp*. 2018;39(1):145–156.
65. Chen X, Zhang H, Zhang L, Shen C, Lee SW, Shen D. Extraction of dynamic functional connectivity from brain grey matter and white matter for MCI classification. *Human Brain Mapp*. 2017;38(10):5019–5034.
66. Chen N, Cai P, Zhou T, Thompson B, Fang F. Perceptual learning modifies the functional specializations of visual cortical areas. *Proc Natl Acad Sci USA*. 2016;113(20):5724–5729.
67. Law CT, Gold JI. Neural correlates of perceptual learning in a sensory-motor, but not a sensory, cortical area. *Nat Neurosci*. 2008;11(4):505–513.
68. Fiorentini A, Berardi N. Perceptual learning specific for orientation and spatial frequency. *Nature*. 1980;287(5777):43–44.
69. Fiorentini A, Berardi N. Learning in grating waveform discrimination: specificity for orientation and spatial frequency. *Vision Res*. 1981;21(7):1149–1158.
70. Poggio T, Fahle M, Edelman S. Fast perceptual learning in visual hyperacuity. *Science*. 1992;256(5059):1018–1021.
71. Barollo M, Contemori G, Battaglini L, Pavan A, Casco C. Perceptual learning improves contrast sensitivity, visual acuity, and foveal crowding in amblyopia. *Restor Neurol Neurosci*. 2017;35(5):483–496.
72. McGovern DP, Webb BS, Peirce JW. Transfer of perceptual learning between different visual tasks. *J Vis*. 2012;12(11):4.
73. Ahissar M, Hochstein S. The reverse hierarchy theory of visual perceptual learning. *Trends Cogn Sci*. 2004;8(10):457–464.
74. Liu Z, Weinshall D. Mechanisms of generalization in perceptual learning. In: *Advances in Neural Information Processing Systems*. Vol 11. MIT Press; 1998. Available at: https://papers.nips.cc/paper_files/paper/1998/hash/46031b3d04dc90994ca317a7c55c4289-Abstract.html. Accessed January 7, 2026..
75. Meyerhoff HS, Papenmeier F, Huff M. Studying visual attention using the multiple object tracking paradigm: a tutorial review. *Atten Percept Psychophys*. 2017;79(5):1255–1274.
76. Culham JC, Brandt SA, Cavanagh P, Kanwisher NG, Dale AM, Tootell RBH. Cortical fMRI activation produced by attentive tracking of moving targets. *J Neurophysiol*. 1998;80(5):2657–2670.
77. Contemori G, Maniglia M, Guénot J, et al. tRNS boosts visual perceptual learning in participants with bilateral macular degeneration. *Front Aging Neurosci*. 2024;16:1326435.
78. Binns AM, Bunce C, Dickinson C, et al. How effective is low vision service provision? A systematic review. *Surv Ophthalmol*. 2012;57(1):34–65.
79. Raphanel M, Shaughness G, Seiple WH, Arleo A. Current practice in low vision rehabilitation of age-related macular degeneration and usefulness of virtual reality as a rehabilitation tool. *J Aging Sci*. 2018. doi:10.4172/2329-8847.1000194.